Molecular Biology of the Cell
Vol. 14, 4770–4782, December 2003

Sec3p Is Needed for the Spatial Regulation of Secretion and for the Inheritance of the Cortical Endoplasmic Reticulum[V]

Andreas Wiederkehr,*† Yunrui Du, †‡ Marc Pypaert,* Susan Ferro-Novick,‡ and Peter Novick*§

*Department of Cell Biology and ‡Howard Hughes Medical Institute, Yale University School of Medicine, New Haven, Connecticut 06510

Submitted April 15, 2003; Revised July 9, 2003; Accepted July 28, 2003
Monitoring Editor: David Drubin

Sec3p is a component of the exocyst complex that tethers secretory vesicles to the plasma membrane at exocytic sites in preparation for fusion. Unlike all other exocyst structural genes, *SEC3* is not essential for growth. Cells lacking Sec3p grow and secrete surprisingly well at 25°C; however, late markers of secretion, such as the vesicle marker Sec4p and the exocyst subunit Sec8p, localize more diffusely within the bud. Furthermore, *sec3*Δ cells are strikingly round relative to wild-type cells and are unable to form pointed mating projections in response to α factor. These phenotypes support the proposed role of Sec3p as a spatial landmark for secretion. We also find that cells lacking Sec3p exhibit a dramatic defect in the inheritance of cortical ER into the bud, whereas the inheritance of mitochondria and Golgi is unaffected. Overexpression of Sec3p results in a prominent patch of the endoplasmic reticulum (ER) marker Sec61p-GFP at the bud tip. Cortical ER inheritance in yeast has been suggested to involve the capture of ER tubules at the bud tip. Sec3p may act in this process as a spatial landmark for cortical ER inheritance.

INTRODUCTION

The genetic dissection of membrane traffic in *Saccharomyces cerevisiae* has facilitated our understanding of the molecular mechanism of vesicular transport. At the post-Golgi stage of the exocytic pathway, more than a dozen gene products are required for the different steps of the transport reaction. The rab GTPase Sec4p and its nucleotide exchange factor Sec2p are required for the polarized delivery of secretory vesicles to sites of secretion (Walch-Solimena *et al*., 1997). This transport step uses actin cables and the type V myosin motor Myo2p (Johnston *et al*., 1991; Govindan *et al*., 1995; Pruyne *et al*., 1998). Actin cables are oriented toward sites of active surface growth. These are the bud tip, early in the yeast cell cycle, and the mother-bud neck, late in the cycle (Adams and Pringle, 1984). After delivery to sites of surface growth, secretory vesicles fuse with the plasma membrane in a reaction mediated by a soluble *N*-ethylmaleimide-sensitive factor attachment protein receptor (SNARE) complex consisting of the yeast t-SNAREs Sso1/2p and Sec9p, together with the v-SNARE Snc1/2p (Brennwald *et al*., 1994; Grote *et al*., 2000). Most of the other gene products required for post-Golgi membrane traffic are components of a large, evolutionarily conserved complex called the exocyst (TerBush *et al*., 1996). The exocyst is composed of eight subunits: Sec3p, Sec5p, Sec6p, Sec8p, Sec10p, Sec15p, Exo70p, and Exo84p. It acts after polarized vesicle delivery, but before SNARE complex formation and fusion (Walch-Solimena *et al*., 1997; Grote *et al*., 2000). The molecular aspects of its role in exocytosis are not fully understood; however, several lines of evidence support a model in which the exocyst acts to tether secretory vesicles to specialized exocytic sites on the plasma membrane before docking and fusion (Guo *et al*., 1999).

The exocyst is peripherally associated with the plasma membrane (Bowser *et al*., 1992), highly concentrated at sites of cell surface growth (TerBush and Novick, 1995; Finger *et al*., 1998). In the case of Sec3p, this polarized localization is independent of the secretory pathway. Sec3p has therefore been postulated to function as a spatial landmark, marking exocytic sites. The localization of Sec3p is dependent on a direct interaction with the Rho1p (Guo *et al*., 2001) and Cdc42p GTPases (Zhang *et al*., 2001), as well as an interaction with Bud4p (Osman *et al*., 2002), but is independent of the actin cytoskeleton (Finger *et al*., 1998). In contrast, another subunit of the exocyst, Sec8p requires both ongoing secretion (Finger *et al*., 1998) and a functional cytoskeleton (Ayscough *et al*., 1997) for its localization. A third subunit, Sec15p associates with secretory vesicles and directly interacts with Sec4p in its GTP-bound form (Guo *et al*., 1999). The working hypothesis is that the exocyst complex assembles as vesicles carrying Sec4p-GTP arrive at sites marked by Sec3p. The assembled complex then acts to tether incoming vesicles to these exocytic sites. We show here that *SEC3* is unique among the exocyst genes in that it is not essential for growth or secretion. Phenotypic analysis of *sec3*Δ cells strongly sup-

Article published online ahead of print. Mol. Biol. Cell 10.1091/mbc.E03–04–0229. Article and publication date are available at www.molbiolcell.org/cgi/doi/10.1091/mbc.E03–04–0229.

† These authors contributed equally to this study.

[V] Online version of this article contains supplementary video materials for some figures. Online version is available at www.molbiolcell.org.

§ Corresponding author. E-mail address: peter.novick@yale.edu.

Abbreviations used: RFP, red fluorescent protein; SC, synthetic complete; YPD, yeast extract peptone dextrose.

Table 1. Yeast strains

Strain	Genotype
NY2448	*Matα sec3Δ::kanMX leu2-3, 112 ura3-52 his3Δ200*
NY2449	*Matα leu2-3, 112 ura3-52 his3Δ200*
NY2450	*Mat***a** *sec3Δ::kanMX leu2-3, 112 ura3-52 his3Δ200*
NY2451	*Matα sec3Δ::kanMX BGL2HA:His5p leu2-3, 112 ura3-52 his3Δ200*
NY2452	*Matα BGL2HA:His5p leu2-3, 112 ura3-52 his3Δ200*
NY2453	*Mat***a** sec3Δ*::kanMX SEC8-GFP:URA3 leu2-3, 112 ura3-52*
NY2454	*Mat***a** *SEC8-GFP:URA3 leu2-3, 112 ura3-52*
NY2463	*Matα sec3Δ::kanMX leu2-3, 112 ura3-52 pNRB807 (2μSEC3:URA3)*
SFNY1056	*Matα SEC61-GFP:LEU2 leu2-3, 112 ura3-52 his3Δ200*
SFNY1153	*Matα sec3Δ::kanMX leu2-3, 112 ura3-52::hmg1-GFP:URA3 his3Δ200*
SFNY1154	*Mat***a** *sec3Δ::kanMX leu2-3, 112 ura3-52::hmg1-GFP:URA3 his3Δ200*
SFNY1162	*Matα leu2-3, 112 ura3-52::hmg1-GFP:URA3 his3Δ200*
SFNY1163	*Mat***a** *leu2-3, 112 ura3-52::hmg1-GFP:URA3 his3Δ200*
SFNY1185	*Matα sec3Δ::kanMX SEC61-GFP:LEU2 leu2-3, 112 ura3-52*

ports the proposed role for Sec3p as a spatial landmark for exocytosis.

A prior study has shown that certain *sec3* mutants seem to accumulate endoplasmic reticulum (ER) tubules in addition to secretory vesicles (Finger and Novick, 1997). Biochemical analysis of these mutants, however, showed no defect at the level of ER-to-Golgi transport and only a minor defect in transport out of the Golgi (Finger and Novick, 1997). A recent study on the dynamics of ER in yeast has offered a possible clue to the cause of this phenotype (Fehrenbacher *et al*., 2002). The ER in yeast is found in a cortical network that makes several tubular connections to the nuclear envelope. At an early stage of bud growth, ER tubules move to the apical tip of the bud and seem to become attached to the cortex at that site. It was proposed that this attachment could direct the inheritance of ER by serving to pull tubules into the bud as the cell cycle progresses (Fehrenbacher *et al*., 2002). Given the proposed role of Sec3p as a spatial landmark for exocytosis as well as the appearance of ER accumulation in *sec3* mutant cells, we explored the possibility that the apical concentration of Sec3p may function as an attachment site for cortical ER. Indeed, we show here that *sec3*Δ mutant cells exhibit a dramatic defect in ER inheritance. By tethering both secretory vesicles and cortical ER, Sec3p may help to orient the entire secretory pathway and thereby facilitate polarized growth.

MATERIALS AND METHODS

Yeast Strains, Media, and Reagents

S. cerevisiae strains used in this study are listed in Table 1. YPD (rich medium) and SD (synthetic medium) were prepared as described previously (Sherman, 1991). For SC media, 40 μg/ml adenine, 20 μg/ml histidine, 40 μg/ml leucine, 40 μg/ml lysine, 20 μg/ml methionine, 10 μg/ml tyrosine, and 40 μg/ml uracil were added. Synthetic complete medium lacking sulfate (SC-S) was prepared similar to the SC medium but all sulfate salts were replaced with the corresponding chloride salts and no methionine was added. To select for cells containing a *URA3* marker based plasmid uracil was omitted from the SC medium. For all experiments described here the strains were grown in SC medium at 25°C overnight to an OD_{600} of 0.2–0.5.

ProMix (Amersham Biosciences, Piscataway, NJ) was used for the ^{35}S-labeling experiments. For the immunoprecipitation of Bgl2HA we used the monoclonal antibody12CA5 and protein G-Sepharose beads (Amersham Biosciences). The enzyme to degrade the yeast cell wall was Zymolyase 100T from Seikagaku America (Rockville, MD). All lysates were prepared in the presence of protease inhibitors 6 μg/ml antipain, 2 μg/ml aprotinin, 2 μg/ml chymostatin, 8 μg/ml leupeptin, 12 μg/ml pepstatin A, and 1 mM phenylmethylsuflonyl fluoride (Sigma-Aldrich, St. Louis, MO).

Strain Construction and Molecular Biology Techniques

Standard techniques were used for the sporulation and the tetrad and complementation analysis of yeast strains (Sherman, 1991). To transform yeast cells a lithium acetate method was used (Gietz *et al*., 1992). Heterozygous diploids were constructed in our strain background by replacing one copy of the exocyst genes with the kanMX-module. The kanMX cassette together with 200–300 base pairs homologous to the 5′ and 3′ region of the disrupted gene was amplified by polymerase chain reaction (PCR) from strains of the yeast deletion collection (ResGen; Invitrogen, Carlsbad, CA). To serve as a template the cells were treated with Zymolyase 100T 120 units/ml for 15 min at 37°C. The cells were harvested at low speed in a bench top microcentrifuge and heated for 5 min at 92°C. The pellets were resuspended in a standard PCR reaction mixture containing the corresponding 3′ and 5′ primers (20mers). After transformation of the PCR products the yeast cells were recovered 3 h in liquid YPD medium at 25°C and then spread onto YPD plates containing 300 μg/ml geneticin (Invitrogen) as the selective antibiotic. For single step chromosomal tagging of *BGL2* the vector pFA6a-3HA-His3MX6 (Longtine *et al*., 1998) was chosen. Long oligonucleotide primers (65 bp) with 45-bp homology to the 3′ end of *BGL2* were designed to remove the stop codon of *BGL2* and fuse in frame the hemagglutinin (HA) tag as described previously (Longtine *et al*., 1998).

To tag the genomic copy of *SEC61* with GFP, the last 576 base pairs of *SEC61*-coding sequence, the coding sequence of GFP (S65G, S72A) (Cormack *et al*., 1997), and the first 455 base pairs of the 3′ noncoding sequence of *SEC61* were amplified by PCR by using the primer pairs pSEC61–1/pSEC61-2 (5′-C A A C G C G G A T C C A A C A C C C C A A T C A T G T T G C A G A G T-3′/5′-C A G T G A A T A A T T C T T C A C C T T T A G A C A T C A A A T C A G A A A A T C C T G G A A C G-3′), pSEC61–3/pSEC61-4 (5′-C G T T C C A G G A T T T T C T G A T T T G A T G T C T A A A G G T G A A G A A T T A T T C A C T G-3′/5′-C T T T G G G A T A T T A T T T T C A T T T T A T A T T C A T T T G T A C A A T T C A T C C A T A C C A T G G-3′), and pSEC61–5/pSEC61-6 (5′-C C A T G G T A T G G A T G A A T T G T A C A A A T G A A T A T A A A A T G A A A A T A A T A T C C A A A G-3′/5′-C A A C G C G G A T C C A T C C G T C C G G A A A A G A G A G C A G A A-3′), respectively. These three fragments served as templates for the fusion PCR by using pSEC61-1 as the 5′ outer oligo, pSEC61-6 as the 3′ outer oligo, and pSEC61-3 as the linking oligo. The PCR product, a fusion of the 3′ part of *SEC61*-coding sequence, the in-frame green fluorescent protein (GFP) sequence and the *SEC61* terminator, was digested with *Bam*HI and subcloned into pRS305, a yeast integrating vector containing *URA3*. The resulting plasmid, pYDY101, was cut at a unique PmlI site within the *SEC61*-coding sequence and used for yeast transformation. The construct was verified by sequencing.

Plasmids expressing the Sec3pΔN and Sec3pΔC regions tagged with four HA epitopes were constructed as follows: first, a plasmid was made by replacing the 1.4-kb *Hind*III-*Kpn*I region in 3ScaI-ApaIpNB419 (Finger and Novick, 1997) with the 1.6-kb *Hind*III-*Kpn*I fragment of pSEC3-4 × HA (Finger *et al*., 1998). The resulting plasmid was then used as template for PCR amplification. The Sec3pΔN-expressing plasmid pGPD-SEC3ΔN-4 × HA was generated by inserting the PCR product, which carries an ATG codon followed by the in-frame 3′ end of the SEC3-4 × HA gene into the p415GPD vector (American Type Culture Collection, Manassas, VA). The Sec3pΔC-expressing plasmid pGPD-SEC3ΔC-4 × HA was generated by inserting the PCR product, which contains the 5′ end of the SEC3 gene and the PCR product that carries the in-frame four consecutive HA epitopes into the p415GPD vector (American Type Culture Collection).

Detailed description of the constructs used for the in vivo localization of different organelles can be found in the following publications: pRH475 carrying the ER marker *hmg1-GFP* (Cronin *et al*., 2000), *SEC7-3 × GFP* as a Golgi marker (Rossanese *et al*., 2001), and pYDY104 for the mitochondrial targeting of red fluorescent protein (mito-RFP; Du *et al*., 2001).

Invertase Secretion

Yeast cells were grown at 25°C to an OD_{600} of 0.2–0.5 in SC medium (2% glucose). Ten OD_{600} units of cells were harvested and washed in 5 ml of SC medium containing only 0.1% glucose. The cell pellet was resuspended in SC 0.1% glucose at 1 OD_{600} unit of cells per milliliter to induce expression of invertase. At several time points after invertase derepression, samples of 1 ml were taken. After the addition of 20 mM sodium azide, these samples were kept on ice. At the end of the time course, the cells were pelleted, washed three times, and resuspended in ice-cold distilled water containing 10 mM sodium azide. Half of the cell suspension was used to determine the extracellular invertase activity. The other half was lysed by two freeze thaw cycles in liquid nitrogen in the presence of 1% Triton X-100. These permeabilized cells were used to determine total cellular invertase activity. Invertase activity was measured as described previously (Goldstein and Lampen, 1975).

Pulse Chase Analysis of Proteins Secreted into the Medium

Cells were grown overnight to OD_{600} of 0.2–0.5 in SC medium at 25°C. The cells were harvested and washed twice in SC-S. The cells were resuspended in SC-S at 2×10^8 cells/ml and incubated for another 10 min at 25°C. Per time point 100 μCi of labeling mixture (ProMix) containing [^{35}S]methionine and [^{35}S]cysteine was added. During the 5-min labeling, the cells were either kept at 25°C or shifted to 37°C. Labeled cells were chased by adding cold methionine, cysteine, and ammonium sulfate to a final concentration of 0.2, 0.25, and 3 mM, respectively. Aliquots of 400 μl of cell suspension were removed during the chase and combined with 10 μl of 1 M sodium azide, 10 μl of 1 M sodium fluoride and kept on ice. The cells were then pelleted at low speed in a Benchtop microcentrifuge at 4°C. To completely remove the cells this step was repeated. Supernatants were transferred to fresh tubes containing trichloroacetic acid (TCA) (final concentration 10%) and deoxycholate (final concentration 0.01%). These samples were incubated on ice for at least 30 min. The proteins were precipitated at 4°C (high-speed centrifugation in Benchtop centrifuge for 10 min). TCA-precipitated proteins were washed twice with acetone at −20°C, air dried, and resuspended in SDS sample buffer (100 mM Tris pH 6.8 2% SDS, 10% glycerol, 3% 2-mercaptoethanol, 0.005% bromphenol blue). Samples were boiled for 5 min and electrophoresed on 8% polyacrylamide gels.

Secretion of Bgl2HA

Wild-type and sec3Δ cells expressing an HA-tagged version of Bgl2p were grown to an OD_{600} of 0.2–0.5. Labeling of these cells was carried out as described above except that 200 μCi of ^{35}S labeling mixture was used per time point. Labeled cells and a 2 times concentrated spheroplast buffer stock were combined to obtain cell suspensions in 100 mM Tris, pH 7.4, 1.4 M sorbitol, 10 mM sodium azide, 10 mM sodium fluoride, 30 mM β-mercaptoethanol, and 0.05 mg/ml Zymolyase. Cell suspensions were incubated for 30 min at 37°C. The released cell wall material was then separated from intact cells by centrifugation. The supernatants were boiled for 5 min after the addition of 1% SDS. For immunoprecipitation the samples were diluted 20-fold with IP-buffer (50 mM HEPES, pH 7.4, 150 mM KCl, 1 mM EDTA, 0.1% βME, 0.5% IGEPAL, and protease inhibitors). Bgl2HA was immunoprecipitated using the 12CA5 monoclonal antibody.

Localization Analysis

In vivo localization of Hmg1p-GFP, Sec7p-GFP, and mitochondrial RFP was performed as described previously (Du *et al*., 2001; Rossanese *et al*., 2001).

For Sec8-GFP localization 4–8 OD_{600} units of yeast cells were harvested and resuspended in 1 ml of fresh SC medium and further incubated at 25°C or shifted to 37°C. After various incubation times the cells were centrifuged in a Benchtop microcentrifuge at low speed for 30 s at room temperature. The cell pellet was immediately fixed in cold methanol and incubated at −20°C for 10 min. After a centrifugation step, the cells were briefly resuspended in cold acetone. The fixed cells were washed three times in phosphate buffered saline before analysis under the fluorescence microscope.

For Sec4p immunofluorescence, yeast cells were grown to an optical density of OD_{600} 0.2–0.5 in SC medium. Aliquots of 20 ml were added to 2.5 ml of 1M KPO_4 pH 6.5 buffer. Immediately, 2.5 ml of formaldehyde solution (37%) was added. For fixation the cells were incubated for 2 h at room temperature. The cells were then washed three times in spheroplasting medium 0.1 M KPO_4, pH 6.5, 1.4 M sorbitol (SP). To digest the cell wall, cell suspensions were incubated in SP containing 20 mM βME and 0.2 mg/ml Zymolyase for 30 min at 30°C. The cells were washed twice in SP and then allowed to bind to polylysine coated glass slides. Before adding the primary antibody the cells were blocked in antibody solution (phosphate buffered saline, 1% bovine serum albumin, 0.1% Triton X-100). Monoclonal antibodies to Sec4p were used as the primary antibody followed by a Texas Red-conjugated goat anti-mouse secondary antibody. Stained cells were visualized using the RITC filter set of a fluorescence microscope (Carl Zeiss, Thornwood, NY).

Indirect immunofluorescence staining using HA-specific antibody was performed essentially as described previously (Du *et al*., 2001).

To visualize filamentous actin structures, cells were grown to early exponential phase at 25°C in SC and fixed in SC medium containing 3.7% formaldehyde for 30 min at 25°C. The cells were then stained with 20 U/ml Texas Red-phalloidin (Molecular Probes, Eugene, OR) as described previously (Finger and Novick, 1997).

Electron Microscopy

Yeast cells were grown at 25°C to an OD_{600} of 0.4 in SC medium. The cells were harvested and resuspended in 1.5% $KMnO_4$ and left for 20 min at room temperature. After five washes with distilled water, cells were stained with 2% uranyl acetate for 4 h at room temperature in the dark. The samples were dehydrated by incubation with 50, 70, 95 (2×5 min each) and 100% ethanol (2×15 min). The cells were then washed briefly in acetone before embedding in Spurr resin (Electron Microscopy Science, Fort Washington, PA). For polymerization, the cell pellets in Spurr were cured for 48 h at 80°C. Ultrathin (60-nm) sections were cut on a Reichert ultramicrotome and collected on formvar- and carbon-coated grids. The samples were poststained with 2% uranyl acetate and lead citrate and examined in a Philips Tecnai 12 electron microscope.

RESULTS

Sec3p Is Not Essential for Growth

Sec3p is a protein of 1336 amino acids containing amino- and carboxy-terminal domains separated by a potential coiled-coil domain (amino acids 322–465) (Haarer *et al*., 1996). The C-terminal domain binds to Sec5p, another subunit of the exocyst, whereas the N-terminal domain binds Rho1p and Cdc42p (Guo *et al*., 2001). Cells expressing Sec3p lacking the Rho1p/Cdc42p binding domain grow quite well (Haarer *et al*., 1996; Guo *et al*., 2001). Truncation of the carboxy-terminal domain of Sec3p, results in poor growth on rich medium, yet relatively good growth on synthetic complete medium (Haarer *et al*., 1996; Osman *et al*., 2002). When the *SEC3* promoter is replaced with the regulated *GAL1* promoter, cells are able to grow slowly on repressing medium, suggesting that *SEC3* may not be essential (Finger and Novick, 1997). Nonetheless, the *Saccharomyces* genome database lists *SEC3* as an essential gene.

We have systematically determined whether each member of the exocyst complex is essential for growth. We created heterozygous diploids by disrupting the eight exocyst genes with the kanMX cassette, leaving only the start and stop codons (see MATERIALS AND METHODS). Geneticin-resistant clones were sporulated and >12 tetrads were dissected on SC and YPD medium. Consistent with an essential role for the exocyst in secretion, seven of the eight heterozygous diploids did not give rise to geneticin-resistant haploids after dissection. In contrast, tetrads derived from the *sec3*Δ/*SEC3* diploids gave rise to two wild-type haploids and two slower growing *sec3*Δ*::kanMX* clones on SC media (Figure 1A). At 37°C, the *sec3*Δ cells were tightly blocked in growth. We conclude that, unlike all other exocyst genes, *SEC3* is not essential for growth.

As was shown for certain *sec3* truncations (Haarer *et al*., 1996), *sec3*Δ cells grew better on SC versus YPD medium at 25°C (Figure 1B). After dissection of the *sec3*Δ/*SEC3* strain on YPD only ~20% of the *sec3*Δ spores gave rise to a colony. The first *sec3*Δ colonies were observed only 5 d after dissection (our unpublished data) compared with 3 d on SC medium (Figure 1A). Therefore, SC medium was used in all the experiments described below. The reasons for the observed growth difference of *sec3*Δ cells on SC versus YPD are un-

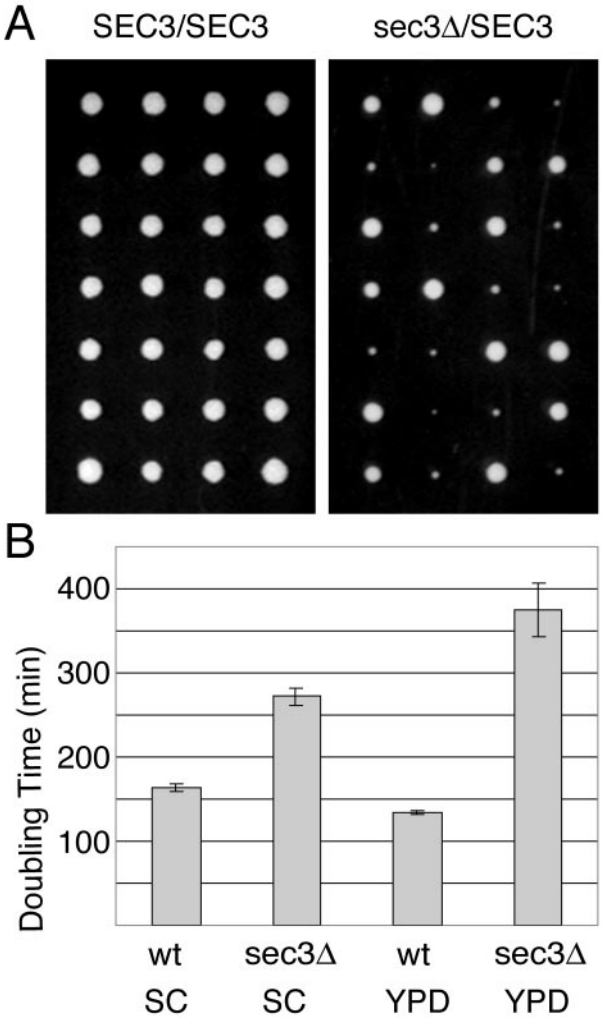

Figure 1. The *SEC3* gene is not essential for yeast growth. (A) A wild-type (left) and heterozygous *sec3*Δ*::kanMX/SEC3* diploid (right) strain were dissected on SC medium at 25°C. Shown are seven tetrads for each strain after 3 d of incubation at 25°C. Each row represents a single tetrad. (B) Wild-type and *sec3*Δ haploid strains were grown overnight in SC or YPD medium. Growth was assessed by measuring the optical density (OD_{600}) after dilution in the indicated medium. Doubling times were calculated from the exponential growth phase. The values shown represent the average doubling times of four wild-type and four *sec3*Δ strains.

clear. The discrepancy with the *Saccharomyces* genome database regarding the essentiality of *SEC3* probably reflects differences in methodology rather than a strain difference because dissection of the heterozygous diploid obtained from the genome project also gave rise to viable *sec3*Δ cells. The sensitivity of *sec3*Δ cells to YPD may explain why disruptants directly selected on YPD geneticin plates were not obtained in the yeast genome project.

*sec3*Δ *Cells Accumulate Only a Small Fraction of Their Secretory Cargo*

To determine the extent to which secretion is inhibited in a *sec3*Δ strain, the export of invertase was monitored at 25°C. In wild-type cells, 90 min after a shift to derepressing medium, only 9.2 ± 3.8% (n = 4) of invertase activity was intracellular (Figure 2A), whereas in *sec3*Δ cells the intracellular pool was 31 ± 2% (n = 4). Given that Sec3p is a subunit of the exocyst, this is a relatively weak effect on secretion. For comparison, several of the temperature-sensitive exocyst mutants accumulate >95% of their invertase in the intracellular pool at their nonpermissive temperature (Novick *et al.*, 1980). At 37°C, >75% of the invertase remained intracellular in *sec3*Δ cells (Figure 2A). Therefore, *sec3*Δ cells are temperature sensitive for both growth and secretion.

The intracellular accumulation of invertase in *sec3*Δ cells at 25°C might indicate a delay rather than a block in secretion. To test this possibility, we followed the release of newly synthesized proteins into the medium by pulse-chase analysis (Figure 2B). Seven minutes (5-min pulse, 2-min chase) after the addition of label, a number of ^{35}S-labeled protein bands were detected in the medium of both wild-type and *sec3*Δ cells. The maximal signal was reached after an 8-min chase, both for wild-type and the *sec3*Δ mutant and the pattern of secreted proteins was similar in both strains. The maximal signal from *sec3*Δ cells was ~30% lower than wild-type even though the incorporation of label into protein was comparable. A possible interpretation of these data is that a fraction of the vesicles is blocked for secretion, whereas the larger fraction is secreted at a rate close to normal. After a shift to 37°C wild-type cells export a somewhat different set of proteins, whereas export from *sec3*Δ cells was almost completely blocked (Figure 2B). The transport block is very rapid, because the *sec3*Δ cells had not been preshifted to 37°C.

In *S. cerevisiae*, newly synthesized secretory proteins are exported via at least two different classes of vesicles that are of similar diameter but differ in their density (Harsay and Bretscher, 1995). Invertase is transported in the denser vesicles, whereas the Bgl2p exoglucanase is found in the lighter vesicles. To assay export of the cargo of the lighter vesicles, we followed an HA-tagged version of Bgl2p by pulse-chase analysis. Wild-type and *sec3*Δ cells synthesized equal amounts of Bgl2HA as determined by immunoprecipitation of ^{35}S-labeled Bgl2HA from total cell lysates (our unpublished data). Bgl2HA was secreted equally well from wild-type and *sec3*Δ cells at 25°C (Figure 2C) and could be detected at the first time point (5-min pulse) in both strains. From these results we conclude that Sec3p is not essential for the export of cargo from either light or dense secretory vesicles.

Spatial Regulation of Exocytosis by Sec3p

During early stages of the cell cycle, growth is restricted to the apical tip of the bud (Adams and Pringle, 1984; Lew and Reed, 1995), and this initial period of apical growth is responsible for the elongated shape of *S. cerevisiae*. Consistent with a defect in the spatial regulation of secretion, *sec3*Δ cells were strikingly round; 80% of the *sec3*Δ, but only 19% of the wild-type cells (n ≥ 200) had an axial ratio <1.1. Because wild-type diploid cells are more elongated than haploid cells, this phenotype was somewhat more exaggerated in diploid cells where 82% of the *sec3*Δ/*sec3*Δ cells and only 6% of the wild-type cells had an axial ratio <1.1.

We determined the effects of the loss of Sec3p on the localization of components of the exocytic machinery. In wild-type, Sec8p-GFP is localized to buds tips and mother-bud necks (Figure 3, A and B, for quantitation). A *sec3*Δ strain with *SEC8-GFP* as its sole copy of *SEC8* grew only slightly slower than the *sec3*Δ mutant. A similar fraction of *sec3*Δ and wild-type cells showed a concentration of Sec8-GFP at the bud tip or neck at 25°C. However, in *sec3*Δ cells,

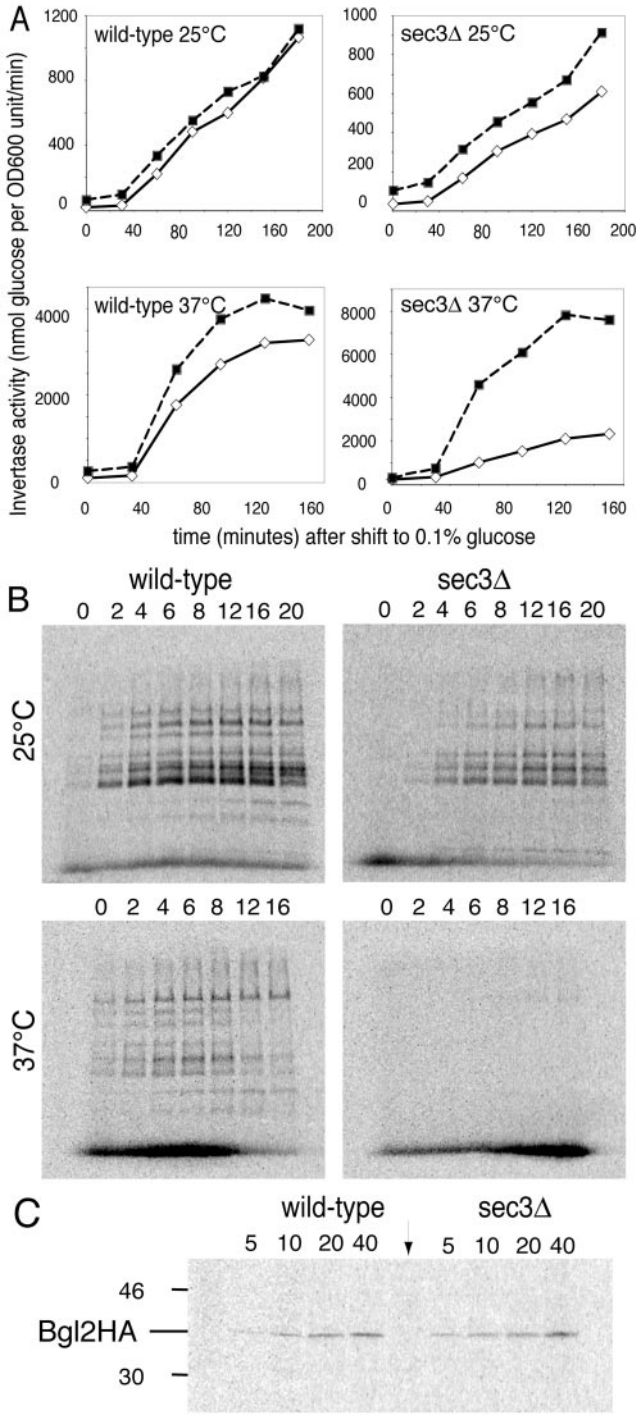

Figure 2. The *sec3*Δ strain has a conditional secretion defect. Wild-type (left) and *sec3*Δ mutant cells (right) were tested for their ability to secrete invertase (A), newly synthesized soluble proteins (B), or Bgl2p, a marker protein for light secretory vesicles (C). For A and B, experiments performed at 25°C (upper) and 37°C (lower) are shown. (A) For invertase secretion assays, the cells were shifted to a low glucose (0.1%) containing medium. Extracellular (white diamonds) and total invertase activity (black squares) were measured. The cells were either continuously grown at 25°C or shifted to 37°C at the 30-min time point. (B) To follow newly synthesized proteins secreted into the medium, cells were labeled for 5 min with ^{35}S labeling mix. The cells were then further incubated in chase medium for the indicated times in min. At the end of the incubation, samples were placed on ice in the presence of 20 mM NaN_3 and 20 mM NaF. Proteins in the cell supernatant were TCA precipitated and electrophoresed on 8% SDS PAGE gels. (C) Bgl2HA was extracted from the extracellular cell wall fraction and then immunoprecipitated as described in the MATERIALS AND METHODS. Pulse-chase analysis was done at 25°C as described in B. The indicated times are minutes after the addition of ^{35}S labeling mix. The lane marked with an arrow is an immunoprecipitate from an untagged wild-type control strain after 20 min of labeling.

the distribution of Sec8-GFP was broader and more background fluorescence was observed in mother cells (Figure 3A).

When shifted to 37°C, wild-type cells lost the bud tip localization of Sec8-GFP within 10 min, whereas bud neck localization was less sensitive to the increase in temperature. After 1 h at 37°C, Sec8-GFP had completely regained its normal distribution (Figure 3, A and B). This behavior may reflect the dependence of Sec8p localization on the actin cytoskeleton, which is also transiently affected by a temperature shift (Delley and Hall, 1999). In *sec3*Δ cells, Sec8-GFP localization was lost from both bud tips and necks after a 10-min shift to 37°C (Figure 3, A and B) and after 1 h only a small number of *sec3*Δ cells were able to repolarize Sec8-GFP (Figure 3, A and B). Thus, at 37°C the localization of the exocyst depends to a large extent on Sec3p.

Using Sec4p as a vesicle marker, we next examined whether secretory vesicles are mistargeted in cells lacking Sec3p. Sec4p is normally concentrated in a small spot at the bud tip (Walch-Solimena *et al*., 1997). At 25°C *sec3*Δ cells showed a much broader distribution of Sec4p than wild-type cells (Figure 4A). Quantification confirmed that the average area of Sec4p staining was 3 to 4 times larger in *sec3*Δ than in wild-type cells (Figure 4B). On the other hand, the average signal intensity in the bud was only slightly higher in the *sec3*Δ cells.

We also examined the role of Sec3p in polarized surface growth after exposure to mating factor. Treatment of *MATa* wild-type cells with α factor resulted in G1 arrest, followed by the growth of a mating projection (Figure 4C). After 4 h of treatment, most cells exhibited a sharply pointed mating projection with Sec4p highly concentrated at the tip. Addition of α factor to *sec3*Δ cells also induced G1 arrest. However the resulting mating projections were predominantly rounded rather than pointed. Sec4p was distributed across the width of the broad mating projections. The average area of Sec4p fluorescence was fourfold greater in *sec3*Δ cells than in wild-type cells. Together, our findings demonstrate that the spatial regulation of secretion is affected in *sec3*Δ strains. Although the overall polarity of surface growth and secretion is maintained in *sec3*Δ strains, the ability to focus surface growth is lost. Therefore, *sec3*Δ strains are deficient in apical growth at the beginning of the cell cycle and are unable to generate pointed projections during the mating response.

*sec3*Δ *Cells Accumulate Exocytic Vesicles and Have Mislocalized Endoplasmic Reticulum*

Electron microscopy can be used to identify the compartment that accumulates in response to a secretory block (Novick *et al*., 1981). As secretory vesicles fuse soon after they are formed, few secretory vesicles can be seen in wild-type cells. As expected from our biochemical analysis, *sec3*Δ cells accumulated secretory vesicles at 25°C (Figure 5C). Vesicles were concentrated preferentially in the bud consis-

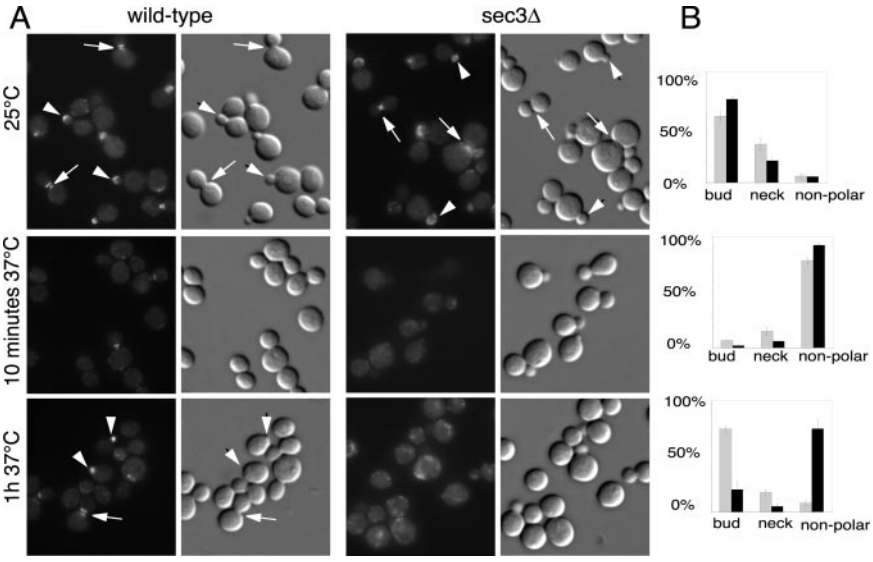

Figure 3. The exocyst subunit Sec8-GFP localizes to buds and bud necks in cells lacking Sec3p.(A) Fluorescence images of Sec8-GFP and corresponding differential interference contrast pictures are shown for wild-type (left) and *sec3*Δ cells (right). Cells were grown at 25°C in SC medium or shifted for the indicated times to 37°C. Examples of cells with bud staining are marked with arrowheads and those with neck staining are marked with arrows. (B) Wild-type (gray bars) and *sec3*Δ cells (black bars) were categorized according to their pattern of Sec8-GFP localization to the bud tip, the bud neck, or delocalized. The graphs depict the percentage of the population within each category. This quantification represents the average from three independent experiments.

tent with the Sec4p localization data. However, a significant number of vesicles were also found in mother cells.

In a prior study, we noted an increase in cytoplasmic ER tubules in two *sec3* alleles, *sec3-4* and *sec3-5* (Finger and Novick, 1997). Although the overall amount of ER and its ultrastructure seemed normal in *sec3*Δ cells, the subcellular localization of the ER was altered (Figure 5, C and D). In wild-type cells, fixed under the conditions used here, the cortical ER is apparent as narrow, darkly stained structures closely apposed to the plasma membrane in both mother cells and buds (Figure 5, A and B). In the *sec3*Δ strain, mother cells exhibited normal cortical ER; however, an increased number of ER tubules were visible in the cytoplasm, often clustered near the nucleus (Figure 5D). Little or no ER was apparent near the cortex of buds (Figure 5, C and D). Quantification showed that 94% (n = 33) of wild-type cells had cortical ER in the bud, whereas only 33% (n = 30) of *sec3*Δ cells had cortical ER in the bud and 27% of *sec3*Δ cells showed a cluster of ER tubules near the nucleus.

Cortical ER Inheritance Is Defective in sec3Δ Cells

Because it can be difficult to interpret the full three-dimensional structure of an extended object, such as the ER, from an electron micrograph, we addressed the relationship between the loss of Sec3p and the change in ER localization by fluorescence microscopy, collecting images at a series of focal planes. We compared the localization of the ER marker Hmg1p-GFP [NH_2-terminal transmembrane domains of

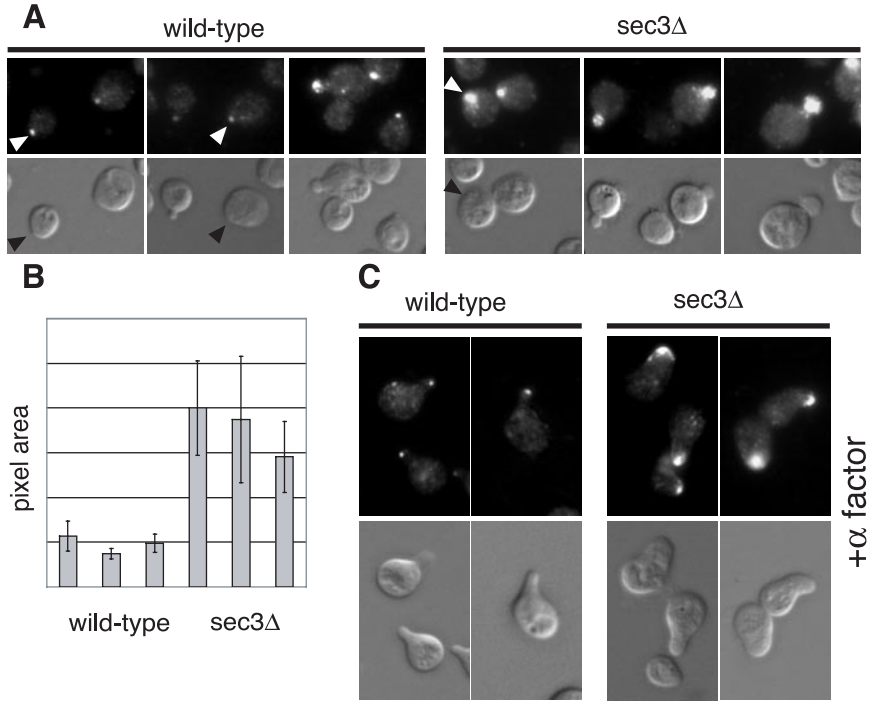

Figure 4. Defect of apical growth in *sec3*Δ cells during early bud growth and shmoo formation. Immunofluorescence of Sec4p (A and C, top) in wild-type (left) and *sec3*Δ cells (right). Corresponding differential interference contrast is shown in the bottom panels. (A) Sec4p is concentrated at incipient bud sites (arrowheads) and in small and medium sized buds. (B) The Sec4p positive area in yeast buds was measured using NIH Image. For this analysis three wild-type and *sec3*Δ clones, obtained after dissection from the same heterozygous diploid were analyzed. The different clones were grown, fixed, and stained in parallel as described in MATERIALS AND METHODS. (C) Sec4p localizes to areas of cell surface growth during shmoo formation. Wild-type (left) and *sec3*Δ cells (right) were treated with 1 μM α factor for 4 h at 25°C.

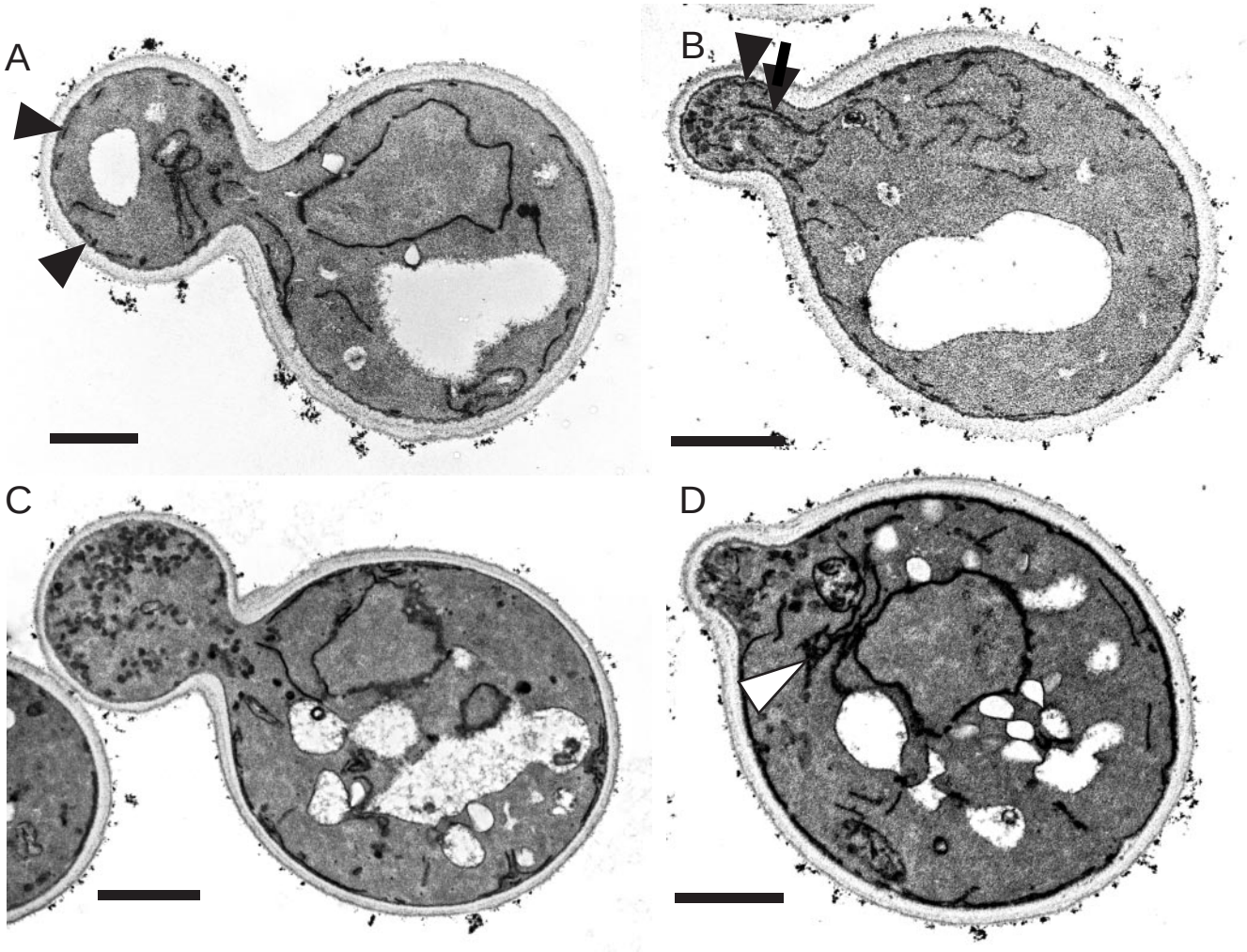

Figure 5. The *sec3*Δ cells accumulate secretory vesicles and exhibit mislocalized endoplasmic reticulum. Wild-type (A and B) and *sec3*Δ cells (C and D) grown in SC medium at 25°C were processed for electron microscopy as described in the MATERIALS AND METHODS. Bar, 1 μm. Black arrowheads point to cortical ER in the daughter cells. Note the absence of cortical ER in the large bud of the *sec3*Δ cell (C). ER tubules extending into the bud (arrow) can be seen in B. An example of ER accumulation in the mother of a *sec3*Δ cell is shown in D (white arrowhead).

HMG-CoA reductase isozyme 1 (Hmg1p) fused to GFP] in *sec3*Δ cells with wild type. In wild-type, the ER is seen as a network of interconnected tubules closely apposed to the plasma membrane (cortical ER) and as connections to the outer membrane of the nuclear envelope (perinuclear ER) (Preuss *et al*., 1991; Prinz *et al*., 2000). Cortical ER is inherited into daughter cells at early stages of bud growth, well before the perinuclear ER. The first ER elements detected in the bud are cytoplasmic tubules that are often oriented along the mother-bud axis (Du *et al*., 2001). These ER tubules are frequently directed to the bud tip before they are delivered to the periphery of the bud (Fehrenbacher *et al*., 2002; our unpublished data).

We observed a severe delay in the delivery of cortical ER into *sec3*Δ daughter cells (Figure 6A). Approximately 60% of small buds (diameters between 0.3 and 0.5 of the mother cell) were virtually devoid of ER, whereas >90% of wild-type buds of this size contained ER tubules that were distributed uniformly along the cortex (Figure 6, A and C). In addition, a significant portion (24%) of small buds in the mutant contained a tubular structure across the bud as the only inherited ER element. Most of these tubules were oriented along the mother-bud axis (Figure 6A, b and c). The intensity of these tubules varied from bright, with an intensity similar to that of the cortical ER tubules in the mother cell (Figure 6A, c), to dim, an example of which is shown in the upper left corner of Figure 6A, b. In larger mutant buds (bud bigger than 0.5 of mother cell, but before nuclear segregation), a lower but still significant portion (34%) contained little or no ER, whereas an increased portion (44%) contained only tubular staining along the mother-bud axis. In contrast, 100% of wild-type buds, in this phase of the cell cycle, contained cortical ER that was indistinguishable from the mother cell. In large budded M-phase cells (containing an elongated nucleus that had not yet divided), a pronounced reduction of cortical ER was observed in 63% of the

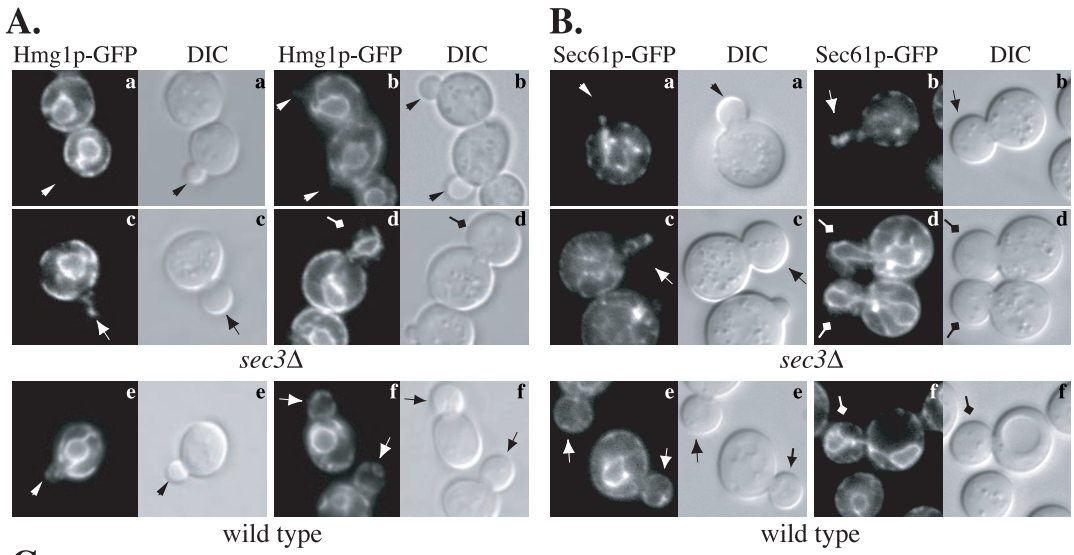

C.

bud category / ER distribution in the bud / strains	small buds			large buds with no nuclei			large buds with undivided nuclei	
	not detectable	only tubules along the axis	tubules at the cortex	not detectable	only tubules along the axis	tubules at the cortex	little or no cortical ER tubules	cortical ER tubules as in the mother cell
SEC3 (Hmg1p-GFP)	1.3% (n=75)	1.3% (n=75)	97% (n=75)	0% (n=43)	0% (n=43)	100% (n=43)	0% (n=52)	100% (n=52)
*sec3*Δ (Hmg1p-GFP)	60% (n=70)	24% (n=70)	16% (n=70)	34% (n=61)	44% (n=61)	21% (n=61)	63% (n=64)	37% (n=64)
SEC3 (Sec61p-GFP)	1.6% (n=62)	3.2% (n=62)	95% (n=62)	0% (n=72)	0% (n=72)	100% (n=72)	0% (n=55)	100% (n=55)
*sec3*Δ (Sec61p-GFP)	51% (n=61)	20% (n=61)	29% (n=61)	27% (n=33)	45% (n=33)	27% (n=33)	66% (n=53)	34% (n=53)

D.

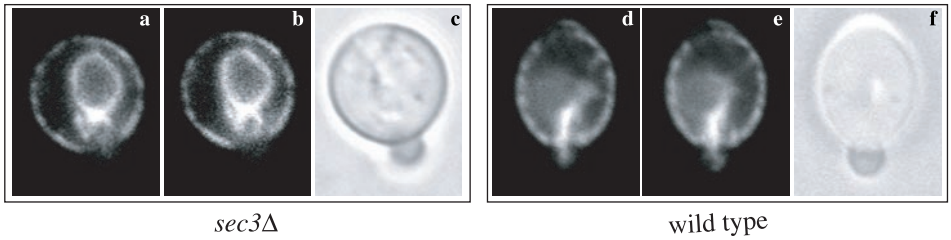

Figure 6. The *sec3*Δ mutant is defective in the inheritance of cortical ER. Hmg1p-GFP (A) and Sec61p-GFP (B) were used as markers to localize the ER in vivo. Fluorescence micrographs of *sec3*Δ (top) and wild-type cells (bottom) are shown. The corresponding differential interference contrast (DIC) pictures show the size of the corresponding yeast buds. The distribution of cortical ER in cells at three different stages of bud formation in *sec3*Δ and wild-type were compared and quantified (C). The three categories were defined as follows (examples of each group are shown in A and B): Small buds between 0.3 and 0.5 times the diameter of the mother cell (arrowheads), buds with a diameter larger than half the mother cell that have not yet received a nucleus (arrows) and large buds where the nucleus has migrated into the bud but is still connected between the mother and daughter cell (diamond arrows). DIC images were taken to measure the diameters of the bud and the mother cells. For each group the fraction of cells with no detectable ER, ER tubules extending into the bud and cortical ER tubules was determined. The number of budded cells examined for each category is indicated in parenthesis. Video supplements to Figure 6A were prepared from z-series images taken at 0.2-μm intervals. (D) Dynamics of Hmg1-GFP labeled ER was monitored by time-lapse imaging. The ER tubule detected in the bud of a *sec3*Δ cell (a) seemed to recede back into the mother cell within 48 s (b). In contrast, ER tubules that were segregated into a wild-type bud (d) were delivered to the bud tip after 48 s (e). The DIC images (c and f) displayed the size of the buds at the beginning of the experiment. Video supplements to Figure 6D were prepared from images collected at 12-s intervals for 10 min.

mutant buds. Faint ER tubules surrounding the perinuclear ER were frequently detected in large *sec3*Δ buds (Figure 6A, d). Before cytokinesis, virtually all *sec3*Δ daughter cells had obtained normal amounts of cortical ER.

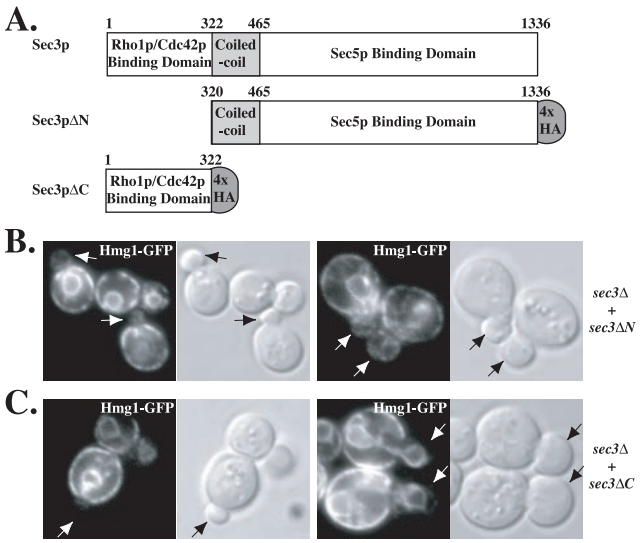

Figure 7. The amino terminal Rho1p binding domain of Sec3p is not required for cortical ER inheritance. (A) Diagram of Sec3p domain structure as well as the Sec3pΔN and Sec3pΔC regions tagged with four HA epitopes (denoted by gray oval). The numeral positions of amino acid residues of Sec3p are indicated. (B and C) Expression of Sec3pΔN but not Sec3pΔC complements the ER inheritance defect of *sec3*Δ cells. ER distribution and differential interference contrast images of representative budded cells (arrows) of a *sec3*Δ strain carrying Sec3pΔN-expressing (B) or Sec3pΔC-expressing (C) plasmids were shown.

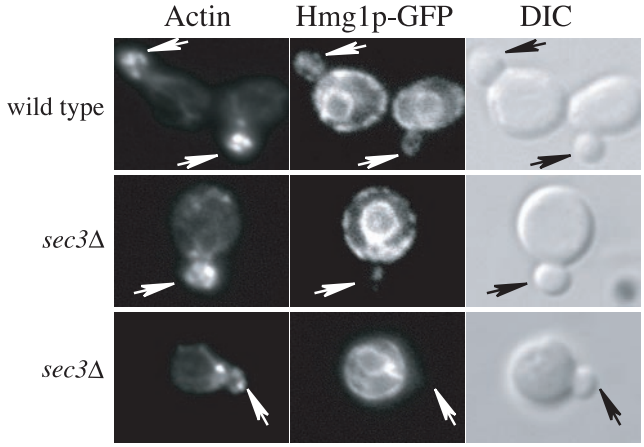

Figure 8. The distribution of the actin cytoskeleton is normal in *sec3*Δ cells. Actin localization in wild-type and *sec3*Δ cells expressing the ER marker Hmg1p-GFP was compared by Texas Red-phalloidin staining. As in wild type, most of the *sec3*Δ cells contain polarized actin patches and cables. Arrows point to the buds.

Time-lapse microscopy demonstrated that, despite the inheritance defect, the ER is still highly dynamic in *sec3*Δ cells (Figure 6D, left). ER tubules marked by Hmg1p-GFP were seen to move toward the neck and often cross into the bud. However, rather than spreading along the cortex, as they do in wild-type (Figure 6D, right), these tubules were often seen to recede back into the mother cell.

To confirm that Sec3p plays a general role in regulating the inheritance of cortical ER rather than a role specific to Hmg1p-GFP, we followed a second ER marker. Sec61p is an ER transmembrane protein required for the translocation and dislocation of proteins across the ER membrane (Johnson and van Waes, 1999). The *SEC61* gene was replaced with a *SEC61-GFP* fusion under the control of the *SEC61* promoter and terminator. Fusion of GFP to the cytosolic COOH terminus (Wilkinson *et al*., 1996) had no obvious effects on cell viability or growth rate. In wild-type, this ER marker showed a localization pattern similar to Hmg1p-GFP (Figure 6B, e and f; and C). In the *sec3*Δ mutant, we noted the accumulation of Sec61p-GFP in the cytoplasm of some cells. Bright spots were also seen in both mother and daughter cells (Figure 6B, a–d). Nevertheless, Sec61p-GFP revealed a significant fraction of *sec3*Δ buds that contained no ER or only tubules along the mother-bud axis. A dramatic decrease of cortical ER was also observed in the large buds of M phase *sec3*Δ cells (Figure 6, B and C). Thus the loss of Sec3p results in a delay in propagating tubules to the bud periphery.

To better define the region of Sec3p needed for ER inheritance, we tested the amino terminal Rho1p binding domain and a *sec3* truncation missing the amino terminal domain for their ability to complement the *sec3*Δ defect (Figure 7A). Expression of the amino terminal domain (Sec3ΔC, residues 1–322) failed to complement the temperature-sensitive growth defect as well as the ER inheritance defect of a *sec3*Δ strain (Figure 7C). In contrast, expression of an allele missing this region (Sec3ΔN, residues 320-1336) complemented both the growth defect and the ER inheritance defect (Figure 7B).

The inheritance defects described could, in principle, be an indirect consequence of accumulating secretory vesicles. To address this possibility, we examined the inheritance of Hmg1p-GFP in another post-Golgi mutant, *sec9-4*, grown at the semirestrictive temperature of 30°C for 12 h before fixation. We chose this temperature because the accumulation of post-Golgi vesicles has been reported in *sec9-4* cells grown at 28.5°C (Finger and Novick, 1997) and the doubling time of the *sec9-4* mutant is increased to a similar degree (2.0 times that of the wild type at 30°C) as that of *sec3*Δ cells at 25°C (1.7 times that of wild type at 25°C). Culturing *sec9-4* cells at 30°C caused abnormal morphologies, such as widened necks and multiple-budded cells, as well as loss of GFP fluorescence in a fraction of the *sec9-4* cells, possibly reflecting cell death. However, under these conditions, ER inheritance occurred normally in >90% (n = 63) of the small budded *sec9-4* cells containing detectable Hmg1p-GFP fluorescence. We have also examined ER inheritance in *sec5-24*, *sec8-9*, *sec10-2*, and *sec15-1* at their semirestrictive temperatures and found it to be normal (our unpublished data). These results imply that impaired post-Golgi secretion does not by itself, cause a delay in cortical ER inheritance.

Actin has been implicated in ER dynamics in yeast (Prinz *et al*., 2000; Fehrenbacher *et al*., 2002). The defect in ER inheritance in *sec3*Δ cells could reflect a defect in actin assembly. We examined the pattern of actin assembly in *sec3*Δ cells at 25°C, yet found it to be normal (Figure 8). Thus, the effects of the loss of Sec3p on ER segregation are not due to the buildup of secretory vesicles or mislocalization of the actin cytoskeleton.

Mitochondria and Golgi Compartments Are Inherited Normally in sec3Δ Cells

In *S. cerevisiae*, mitochondria also form an interconnected tubular network at the cell periphery (Yaffe, 1999). Previous studies have suggested a close association between the ER

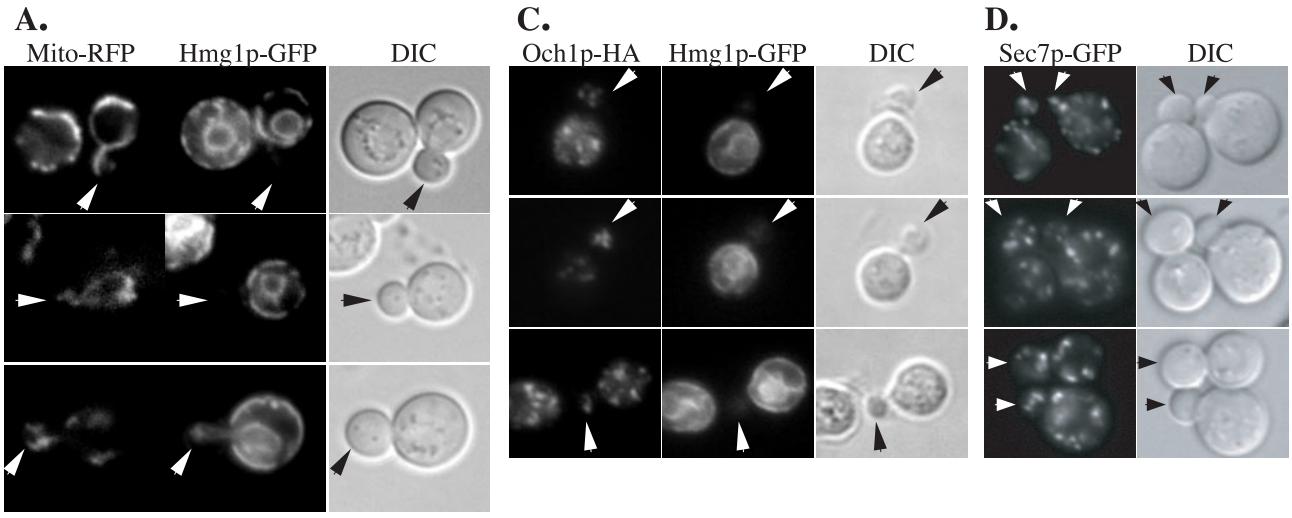

B.

bud category / mitochondria distribution / strains	small buds				large buds with no nuclei				large buds with nuclei			
SEC3	41% (n=73)	29% (n=/73)	30% (n=/73)	0% (n=/73)	9% (n=66)	36% (n=66)	46% (n=66)	9% (n=66)	0% (n=71)	6% (n=71)	45% (n=71)	49% (n=71)
*sec3*Δ	31% (n=83)	39% (n=83)	30% (n=83)	0% (n=83)	6% (n=54)	33% (n=54)	54% (n=54)	7% (n=54)	0% (n=61)	10% (n=61)	34% (n=61)	56% (n=61)

Figure 9. The inheritance of mitochondria, early and late Golgi is not defective in *sec3*Δ cells. (A) *sec3*Δ cells expressing Hmg1p-GFP and RFP fused to a mitochondrial targeting sequence were used to directly compare the inheritance of cortical ER and mitochondria into the bud. (B) Quantification of mitochondrial inheritance into the bud of *sec3*Δ and wild-type cells. The distinction between different bud sizes was made as described in the legend to Figure 6C. Four different types of mitochondrial distributions in the bud can be distinguished (see schematic drawings in the table and Simon *et al.*, 1997). The number in parenthesis indicates the number of cells analyzed. (C) Distribution of the *cis*-Golgi marker Och1p-HA (left) in the bud of *sec3*Δ mutant cells was compared with the localization of Hmg1p-GFP (center). Differential interference contrast pictures of the corresponding cells are shown on the right. Arrows point to mutant buds with no cortical ER. (D). The inheritance and distribution of the late Golgi was normal as shown by the localization of Sec7p-GFP in *sec3*Δ cells.

and mitochondria in both yeast and mammalian cells (Montisano *et al.*, 1982; Perkins *et al.*, 1997; Prinz *et al.*, 2000). Moreover, mitochondria are inherited by transmitting tubules along the mother-bud axis. The tubules become immobilized at the bud tip and are then distributed to the periphery (Simon *et al.*, 1997). To address a possible role of Sec3p in this process, we used a mitochondrial targeting sequence fused to RFP (Du *et al.*, 2001). In wild-type cells, about one-third of small budded cells contained mitochondrial tubules across the bud, but not at the tip, whereas one-third contained mitochondria tubules that had contacted the bud tip (Figure 9B). The rest of the small budded cells contained tubules along the mother-bud axis at the base of the neck. For large budded cells in the late S to G2 phases of the cell cycle, an increased fraction of buds had tubules contacting the tip and ~10% of the buds contained tubules in the cortical region. After cells entered mitosis, mitochondrial tubules were found at the periphery in the majority of the buds, with the same distribution as in the mother cell. When mitochondrial distribution was examined in *sec3*Δ cells, we found that mitochondria tubules were successfully transmitted into the buds that had failed to inherit cortical ER (Figure 9A). Quantification of mitochondrial inheritance in *sec3*Δ cells revealed no delay in transmitting mitochondrial tubules into the bud or in propagating these tubules to the bud periphery (Figure 9B).

We also investigated the inheritance of early and late Golgi membranes in *sec3*Δ cells. Early Golgi membranes have been shown to occur in buds at essentially the same stage of bud growth as cortical ER (Preuss *et al.*, 1992; Du *et al.*, 2001; Rossanese *et al.*, 2001). We followed the distribution of a HA-tagged version of Och1p, an enzyme that defines one of the earliest Golgi compartments in yeast. We analyzed 63 *sec3*Δ mutant cells in which the bud contained no Hmg1p-GFP–labeled ER elements or only ER tubules along the mother-bud axis. All had obtained one to five Och1p-HA–labeled spots, which was comparable with wild-type (Figure 9C). To study the inheritance of late Golgi, we replaced the *SEC7* gene with a *SEC7-GFP* fusion. Sec7p is a peripheral membrane protein that specifically localizes to the late Golgi apparatus (Rossanese *et al.*, 2001). Sec7p-GFP localized to 10–15 spots in wild-type and *sec3*Δ cells (Figure

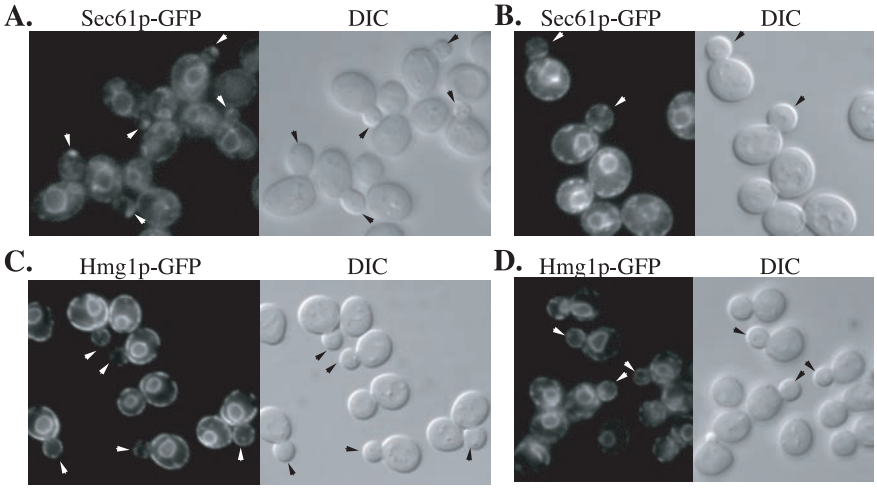

Figure 10. Overexpression of Sec3p leads to an accumulation of Sec61p-GFP but not Hmg1p-GFP at the bud tip. Representative images of Sec61p-GFP (A and B) and Hmg1p-GFP (C and D) in a Sec3p overproducer, NY2463 (*sec3*::kanMX, pRS426-SEC3; A and C) and in a control strain, NY1211 (*SEC3*; B and D) are shown. Arrows point to either small buds or medium-sized buds.

9D). Virtually all (68 of 69) small buds of *sec3*Δ cells acquired one to four Sec7-GFP–labeled spots, which was similar to the distribution in wild type. Therefore, we did not detect any significant defects in the structure or inheritance of either early or late Golgi membranes in *sec3*Δ cells. In total, our results show that Sec3p specifically affects secretory vesicle targeting and ER inheritance.

Overexpression of Sec3p Leads to the Formation of a Cap of Sec61p at Bud Tips

If Sec3p plays a direct role in anchoring the ER at bud tips, overexpression of Sec3p might be expected to alter the distribution of the ER or its binding partner on the ER. Indeed, Sec61-GFP localization exhibited a prominent dot or cap in 89% (n = 117) of small- to medium-sized buds of cells overexpressing Sec3p from a high copy number vector (Figure 10A). In control cells, only 15% of the buds had a dot or cap of Sec61-GFP (Figure 10B). Furthermore, the Sec61-GFP dots or caps were generally much brighter in the Sec3p-overexpressing cells relative to the control. In contrast to Sec61-GFP localization, Hmg1-GFP localization seemed normal in cells overexpressing Sec3p (Figure 10C). Electron microscopy of Sec3p-overexpressing cells revealed no abnormal accumulation of membrane at the tips of buds (our unpublished data). The Sec3p mediated concentration of Sec61-GFP at the bud tip therefore does not reflect a general effect on ER distribution.

DISCUSSION

In a prior study, we had found that the localization of Sec3p to bud tips and necks is maintained even when vesicular transport is blocked or when the actin cytoskeleton is depolymerized (Finger *et al*., 1998). Sec3p was therefore proposed to act as a spatial landmark for polarized secretion. The findings presented here strongly support a model in which Sec3p marks subdomains of the plasma membrane for efficient targeting and tethering of secretory vesicles. Furthermore, we now extend that proposal to include a role for Sec3p, and perhaps other components of the exocyst, as an anchor at the bud tip for ER tubules segregated into daughter cells.

Here, we show that, unlike all other subunits of the exocyst, Sec3p is not essential for growth or for export of secretory cargo. Furthermore, the pattern of actin assembly as well as the actin-dependent polarized transport of secretory vesicles and other organelles looks normal in *sec3*Δ cells. Indeed, the vesicle marker Sec4p and the GFP-tagged exocyst subunit Sec8p are still found concentrated in the bud or close to the mother bud neck under permissive growth conditions. However, in the absence of Sec3p, the vesicles do not seem to find appropriate exocytic sites within the bud, and this results in the fusion of vesicles along the entire surface of the bud. This hypothesis is supported by the broader distribution of Sec4p and the more diffuse localization of Sec8-GFP within the buds of *sec3*Δ cells relative to wild-type buds (Figures 3 and 4). Such delocalized fusion within the bud would lead to isotropic growth and hence explain the observed round morphology of *sec3*Δ cells. A similar situation occurs during the formation of mating projections in response to mating factor. Vesicles marked by Sec4p are still delivered in a polarized manner in *sec3*Δ cells, but rather than fusing within a well focused spot, they fuse along a broad front and thereby give rise to a bulbous mating projection. Inefficient targeting may also lead to the failure of a fraction of the vesicles to fuse, as seen in *sec3*Δ cells under permissive conditions. At 37°C, *sec3*Δ cells, similar to conditional mutants defective in other exocyst components, are tightly blocked for growth, fail to export a large fraction of their secretory cargo and accumulate secretory vesicles in a polarized manner. In addition, the polarized localization of Sec8-GFP is lost after a shift of *sec3*Δ cells to 37°C (Figure 3A). Sec3p may be critical for the stability of the exocyst at 37°C, whereas at 25°C the complex may remain sufficiently assembled or active to mediate its essential functions in exocytosis without Sec3p. Thus, a critical function of Sec3p may be to bind and stabilize the exocyst complex at exocytic sites.

We also report the unexpected finding that Sec3p plays a key role in the inheritance of cortical ER. In *S. cerevisiae*, this seems to be a multistage process involving transport of cytoplasmic ER tubules along the mother-bud axis, followed by their association with the bud tip and then their propagation along the bud cortex (Du *et al*., 2001) (Fehrenbacher *et al*., 2002; our unpublished data). The daughter cell obtains ER tubules at the cortical region early in S phase, shortly after the initiation of bud growth (Preuss *et al*., 1991; Du *et al*., 2001). In contrast, more than half of *sec3*Δ mutant buds fail to acquire ER tubules at their cortex even at late S to G2 phases (Figure 6). Moreover, a significant fraction of *sec3*Δ

cells contains tubules across the bud as the only inherited ER elements. Thus, we speculate that Sec3p marks the bud tip destination for ER tubules, similar to its role as a landmark for secretory vesicles. Electron microscopy revealed that many of the *sec3*Δ cells had an unusually large amount of cytoplasmic ER in the mother cell, in most cases close to the nucleus (Figure 5D), and a similar phenotype had been noted in a study of *sec3-4* and *sec3-5* mutant cells (Finger and Novick, 1997). Because ER to Golgi transport is unaffected in these cells, it is possible that the structures represent ER tubules that have been retracted back into the mother cell after an unsuccessful attempt to associate with the cortex of the bud. Time-lapse microscopy shows that ER tubules are highly dynamic in *sec3*Δ cells. Tubules move across the neck, but fail to be stably retained in the bud. Neither mitochondria nor late Golgi, two other organelles that are transported to the bud tip during the cell cycle (Simon *et al*., 1997; Rossanese *et al*., 2001), require the function of Sec3p for proper inheritance (Figure 9). It therefore seems that the role of Sec3p is limited to the localization of secretory vesicles and ER tubules.

Rho1p acts through at least two pathways to control the localization of the exocyst. The amino terminus of Sec3p has been shown to bind to Rho1p (Guo *et al*., 2001) and an allele of Sec3p deleted for the Rho1p-binding domain (Sec3ΔN-GFP) is mislocalized, but only when expressed in a wild-type *SEC3* background. When expressed as the sole copy, partial localization of Sec3ΔN-GFP is seen and the other subunits of the exocyst still localize quite well (Guo *et al*., 2001) implying a Sec3-independent pathway for exocyst localization. Apparently, the truncated allele of Sec3p can localize to some extent by assembling with the rest of the exocyst. We show here that expression of Sec3ΔN is able to complement the ER inheritance defect of a *sec3*Δ strain. A temperature-sensitive *rho1* mutant does show a partial defect in ER inheritance after a shift to the restrictive temperature (our unpublished observations). A more complete defect is not seen because this allele may be only partially defective for this function, because other Rho family members are partially redundant or because some of the buds contain ER that had been segregated before the temperature shift. In general, it is difficult to assay organelle inheritance in mutants such as *rho1*that are blocked in bud growth.

An important clue to the role of Sec3p in ER inheritance has come from our observation of the effects of Sec3p overexpression. The formation of a prominent patch of Sec61-GFP at the bud tip in response to Sec3p overexpression, without a parallel change in Hmg1-GFP localization or an accumulation of ER membrane suggests that the patch may represent a selective enrichment of Sec61-GFP within the plane of the ER membrane at the bud tip, rather than an actual increase in the amount of ER membrane at this site. Such a selective enrichment could reflect a physical linkage, either direct or through intermediaries, between Sec61-GFP and the exocyst. Both genetic as well as physical interactions have been observed between the exocyst and components of the translocon. *SEB1*, encoding the β subunit of the Sec61 translocon complex, was identified as a high copy number suppressor of *sec15-1* (Toikkanen *et al*., 1996) and was recently shown to suppress defects in the other subunits of the exocyst as well. Overexpression of the other two subunits of the translocon suppresses several exocyst mutants. Coprecipitation experiments indicate a physical linkage between the exocyst and the translocon in both yeast (Toikkanen *et al*., 2003) and mammalian cells (Lipschutz *et al*., 2003). In total, these studies support the proposed physical connection between the exocyst at the apical tip of the plasma membrane and the Sec61p-containing translocon complex on the ER membrane. Although the efficiency of coprecipitation reported was not high, it is consistent with the observation that only a small portion of the ER is actually anchored at the bud tip and that both the translocon and exocyst complexes have other essential functions. Establishing the details of this interaction between two large, multisubunit complexes will require further studies.

Together, our results show that Sec3p is not essential for exocytosis in yeast but is required for tethering secretory vesicles to specialized subdomains of the plasma membrane. In a similar manner, Sec3p is also required to stabilize the cortical association of ER tubules that have been extended into the yeast bud. In this way, Sec3p may initiate ER retention and promote distribution along the cortex of the newly forming bud. The Sec3p mediated connection between cortical ER and exocytosis at the bud tip together with the actin-mediated inheritance of Golgi structures may establish an autonomous secretory apparatus in the daughter cells soon after bud initiation and thereby facilitate polarized growth.

ACKNOWLEDGMENTS

We thank Randy Hampton, Janet Shaw, Benjamin Glick, Gerry Waters, Charles Boyd, and Jeff Coleman for yeast strains and plasmids and Elaine Downie for technical assistance. This work was supported by grants from the National Institutes of Health to P.N (GM35370) and to S.F.N. (CA 46128, project 2). A.W. was supported by a fellowship from the Swiss National Science Foundation. Y.D. is an associate of the Howard Hughes Medical Institute.

REFERENCES

Adams, A.E., and Pringle, J.R. (1984). Relationship of actin and tubulin distribution to bud growth in wild-type and morphogenetic-mutant *Saccharomyces cerevisiae*. J. Cell Biol. *98*, 934–945.

Ayscough, K.R., Stryker, J., Pokala, N., Sanders, M., Crews, P., and Drubin, D.G. (1997). High rates of actin filament turnover in budding yeast and roles for actin in establishment and maintenance of cell polarity revealed using the actin inhibitor latrunculin-A. [published erratum appears in J. Cell Biol. 1999 Sep 6;146(5):following 1201]. J. Cell Biol. *137*, 399–416.

Bowser, R., Muller, H., Govindan, B., and Novick, P. (1992). Sec8p and Sec15p are components of a plasma membrane-associated 19.5S particle that may function downstream of Sec4p to control exocytosis. J. Cell Biol. *118*, 1041–1056.

Brennwald, P., Kearns, B., Champion, K., Keranen, S., Bankaitis, V., and Novick, P. (1994). Sec9 is a SNAP-25-like component of a yeast SNARE complex that may be the effector of Sec4 function in exocytosis. Cell *79*, 245–258.

Cormack, B.P., Bertram, G., Egerton, M., Gow, N.A.R., Falkow, S., and Brown, A.J.P. (1997). Yeast-enhanced green fluorescent protein (yEGFP): a reporter of gene expression in *Candida albicans*. Microbiology *143*, 303–311.

Cronin, S.R., Khoury, A., Ferry, D.K., and Hampton, R.Y. (2000). Regulation of HMG-CoA reductase degradation requires the P-type ATPase Cod1p/Spf1p. J. Cell Biol. *148*, 915–924.

Delley, P.A., and Hall, M.N. (1999). Cell wall stress depolarizes cell growth via hyperactivation of RHO1. J. Cell Biol. *147*, 163–174.

Du, Y., Pypaert, M., Novick, P., and Ferro-Novick, S. (2001). Aux1p/Swa2p is required for cortical endoplasmic reticulum inheritance in *Saccharomyces cerevisiae*. Mol. Biol. Cell. *12*, 2614–2628.

Fehrenbacher, K.L., Davis, D., Wu, M., Boldogh, I., and Pon, L.A. (2002). Endoplasmic reticulum dynamics, inheritance, and cytoskeletal interactions in budding yeast. Mol. Biol. Cell. *13*, 854–865.

Finger, F.P., Hughes, T.E., and Novick, P. (1998). Sec3p is a spatial landmark for polarized secretion in budding yeast. Cell *92*, 559–571.

Finger, F.P., and Novick, P. (1997). Sec3p is involved in secretion and morphogenesis in *Saccharomyces cerevisiae*. Mol. Biol. Cell *8*, 647–662.

Gietz, D., St. Jean, A., Woods, R.A., and Schiestl, R.H. (1992). Improved method for high efficiency transformation of intact yeast cells. Nucleic Acids Res. *20*, 1425.

Goldstein, A., and Lampen, J.O. (1975). Beta-D-fructofuranoside fructohydrolase from yeast. Methods Enzymol. *42*, 504–511.

Govindan, B., Bowser, R., and Novick, P. (1995). The role of Myo2, a yeast class V myosin, in vesicular transport. J. Cell Biol. *128*, 1055–1068.

Grote, E., Carr, C.M., and Novick, P.J. (2000). Ordering the final events in yeast exocytosis [In Process Citation]. J. Cell Biol. *151*, 439–452.

Guo, W., Roth, D., Walch-Solimena, C., and Novick, P. (1999). The exocyst is an effector for Sec4p, targeting secretory vesicles to sites of exocytosis. EMBO J. *18*, 1071–1080.

Guo, W., Tamanoi, F., and Novick, P. (2001). Spatial regulation of the exocyst complex by Rho1 GTPase. Nat. Cell Biol. *3*, 353–360.

Haarer, B.K., Corbett, A., Kweon, Y., Petzold, A.S., Silver, P., and Brown, S.S. (1996). SEC3 mutations are synthetically lethal with profilin mutations and cause defects in diploid-specific bud-site selection. Genetics *144*, 495–510.

Harsay, E., and Bretscher, A. (1995). Parallel secretory pathways to the cell surface in yeast. J. Cell Biol. *131*, 297–310.

Johnson, A.E., and van Waes, M.A. (1999). The translocon: a dynamic gateway at the ER membrane. Annu. Rev. Cell. Dev. Biol. *15*, 799–842.

Johnston, G.C., Prendergast, J.A., and Singer, R.A. (1991). The *Saccharomyces cerevisiae* MYO2 gene encodes an essential myosin for vectorial transport of vesicles. J. Cell Biol. *113*, 539–551.

Lew, D.J., and Reed, S.I. (1995). A cell cycle checkpoint monitors cell morphogenesis in budding yeast. J. Cell Biol. *129*, 739–749.

Lipschutz, J., Lingappa, V., and Mostov, K. (2003). The exocyst affects protein synthesis by acting on the translocon machinery of the endoplasmic reticulum. J. Biol. Chem. *278*, 20954–20960.

Longtine, M.S., McKenzie 3rd, A., Demarini, D.J., Shah, N.G., Wach, A., Brachat, A., Philippsen, P., and Pringle, J.R. (1998). Additional modules for versatile and economical PCR-based gene deletion and modification in *Saccharomyces cerevisiae*. Yeast *14*, 953–961.

Montisano, D.F., Cascarano, J., Pickett, C.B., and James, T.W. (1982). Association between mitochondria and rough endoplasmic reticulum in rat liver. Anat. Rec. *203*, 441–450.

Novick, P., Ferro, S., and Schekman, R. (1981). Order of events in the yeast secretory pathway. Cell *25*, 461–469.

Novick, P., Field, C., and Schekman, R. (1980). Identification of 23 complementation groups required for post-translational events in the yeast secretory pathway. Cell *21*, 205–215.

Osman, M., Konopka, J., and Cerione, R. (2002). Iqg1p links spatial and secretion landmarks to polarity and cytokinesis. J. Cell Biol. *159*, 601–611.

Perkins, G., Renken, C., Martone, M.E., Young, S.J., Ellisman, M., and Frey, T. (1997). Electron tomography of neuronal mitochondria: three-dimensional structure and organization of cristae and membrane contacts. J. Struct. Biol. *119*, 260–272.

Preuss, D., Mulholland, J., Franzusoff, A., Segev, N., and Botstein, D. (1992). Characterization of the *Saccharomyces* Golgi complex through the cell cycle by immunoelectron microscopy. Mol. Biol. Cell. *3*, 789–803.

Preuss, D., Mulholland, J., Kaiser, C.A., Orlean, P., Albright, C., Rose, M.D., Robbins, P.W., and Botstein, D. (1991). Structure of the yeast endoplasmic reticulum: localization of ER proteins using immunofluorescence and immunoelectron microscopy. Yeast *7*, 891–911.

Prinz, W.A., Grzyb, L., Veenhuis, M., Kahana, J.A., Silver, P.A., and Rapoport, T.A. (2000). Mutants affecting the structure of the cortical endoplasmic reticulum in *Saccharomyces cerevisiae*. J. Cell Biol. *150*, 461–474.

Pruyne, D.W., Schott, D.H., and Bretscher, A. (1998). Tropomyosin-containing actin cables direct the Myo2p-dependent polarized delivery of secretory vesicles in budding yeast. J. Cell Biol. *143*, 1931–1945.

Rossanese, O.W., Reinke, C.A., Bevis, B.J., Hammond, A.T., Sears, I.B., O'Connor, J., and Glick, B.S. (2001). A role for actin, Cdc1p, and Myo2p in the inheritance of late Golgi elements in *Saccharomyces cerevisiae*. J. Cell Biol. *153*, 47–62.

Sherman, F. (1991). Getting started with yeast. Methods Enzymol. *194*, 3–21.

Simon, V.R., Karmon, S.L., and Pon, L.A. (1997). Mitochondrial inheritance: cell cycle and actin cable dependence of polarized mitochondrial movements in *Saccharomyces cerevisiae*. Cell Motil. Cytoskeleton *37*, 199–210.

TerBush, D.R., Maurice, T., Roth, D., and Novick, P. (1996). The Exocyst is a multiprotein complex required for exocytosis in *Saccharomyces cerevisiae*. EMBO J. *15*, 6483–6494.

TerBush, D.R., and Novick, P. (1995). Sec6, Sec8, and Sec15 are components of a multisubunit complex which localizes to small bud tips in *Saccharomyces cerevisiae*. J. Cell Biol. *130*, 299–312.

Toikkanen, J., Gatti, E., Takei, K., Saloheimo, M., Olkkonen, V.M., Soderlund, H., De Camilli, P., and Keranen, S. (1996). Yeast protein translocation complex: isolation of two genes SEB1 and SEB2 encoding proteins homologous to the Sec61 beta subunit. Yeast *12*, 425–438.

Toikkanen, J., Miller, K., Soderlund, H., Jantti, J., and Keranen, S. (2003). The beta subunit of the Sec61p ER translocon interacts with the exocyst complex in *Saccharomyces cerevisiae*. J. Biol. Chem. *278*, 20946–20953.

Walch-Solimena, C., Collins, R.N., and Novick, P.J. (1997). Sec2p mediates nucleotide exchange on Sec4p and is involved in polarized delivery of post-Golgi vesicles. J. Cell Biol. *137*, 1495–1509.

Wilkinson, B.M., Critchley, A.J., and Stirling, C.J. (1996). Determination of the transmembrane topology of yeast Sec61p, an essential component of the endoplasmic reticulum translocation complex. J. Biol. Chem. *271*, 25590–25597.

Yaffe, M.P. (1999). The machinery of mitochondrial inheritance and behavior. Science *283*, 1493–1497.

Zhang, X., Bi, E., Novick, P., Du, L., Kozminski, K.G., Lipschutz, J.H., and Guo, W. (2001). Cdc42 interacts with the exocyst and regulates polarized secretion. J. Biol. Chem. *276*, 46745–46750.